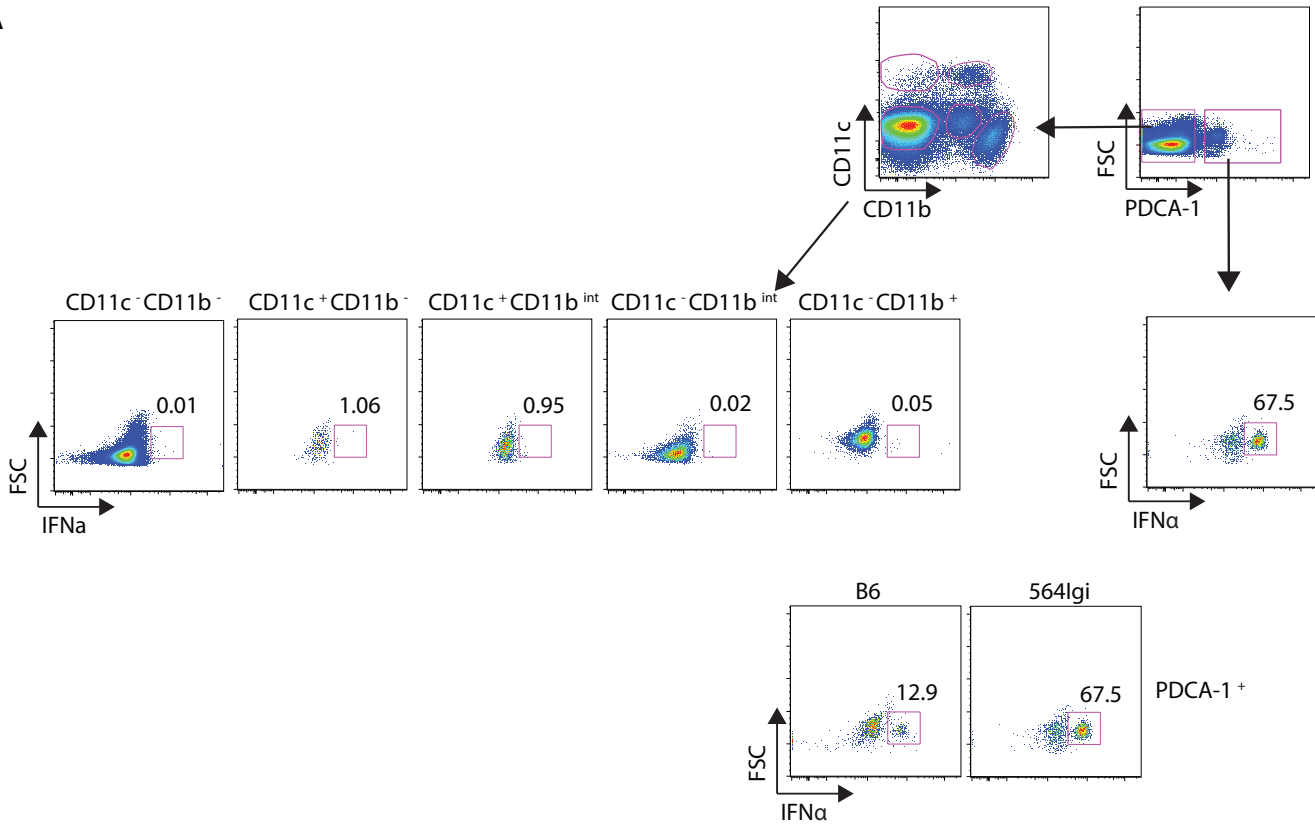
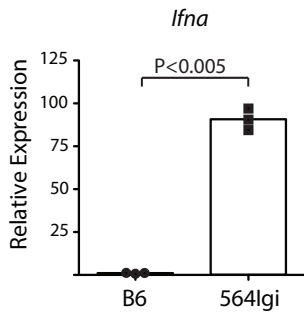


Figure S1

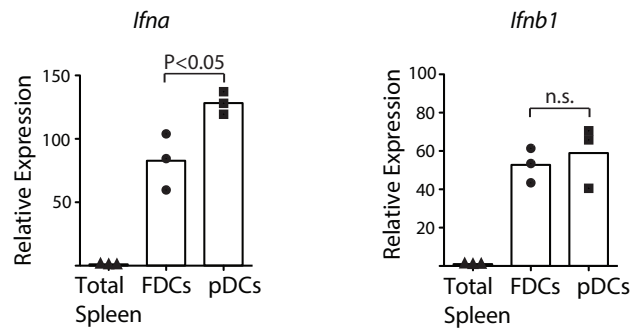
A



B



C



Ct values:	<i>Ifna</i>			<i>Ifnb1</i>		
FDCs	21.6	22.0	22.2	28.3	29.0	28.6
pDCs	20.6	20.5	21.0	29.3	28.7	28.9
Total Spleen	28.6	28.1	28.9	34.6	34.9	34.7

D

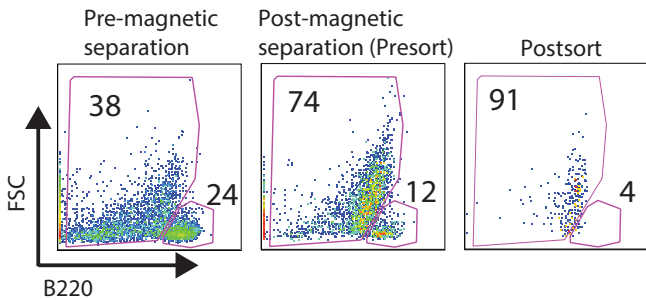


Figure S2

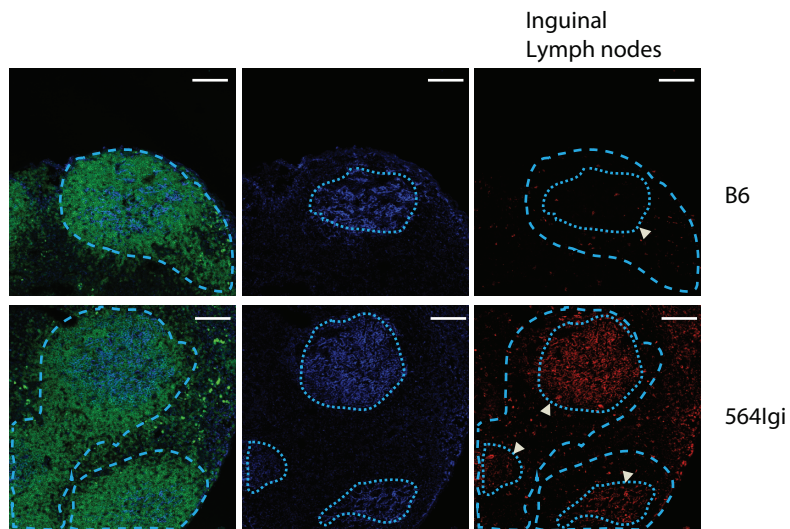
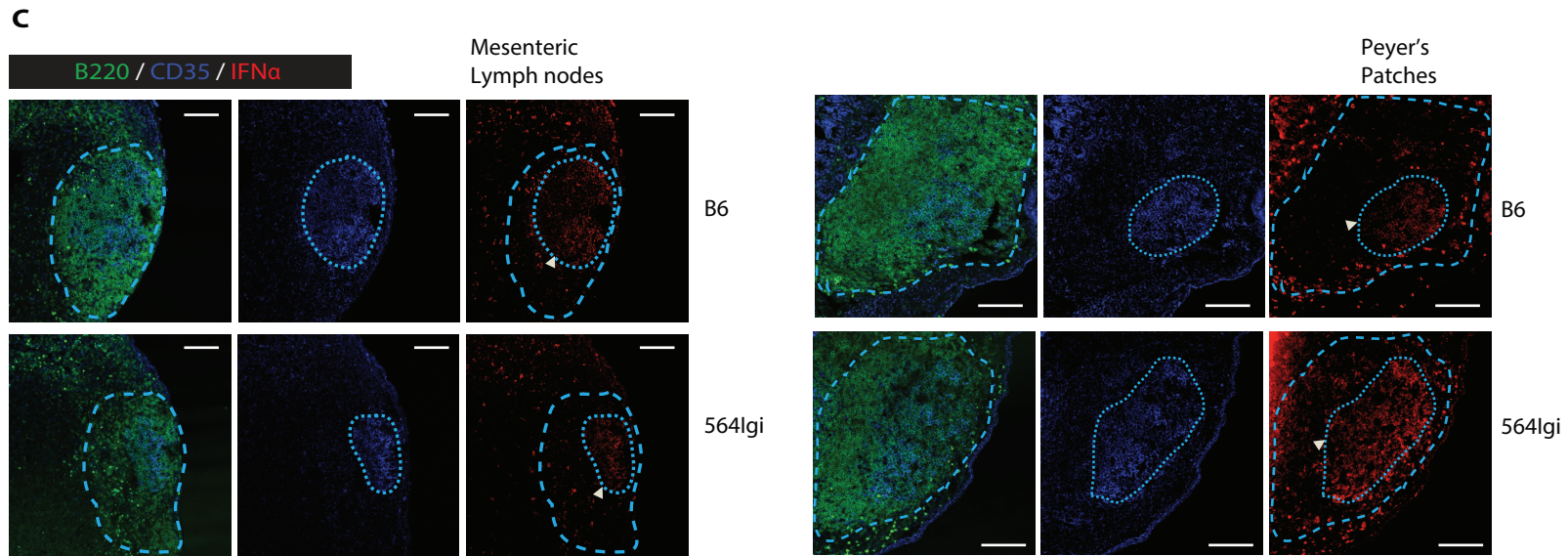
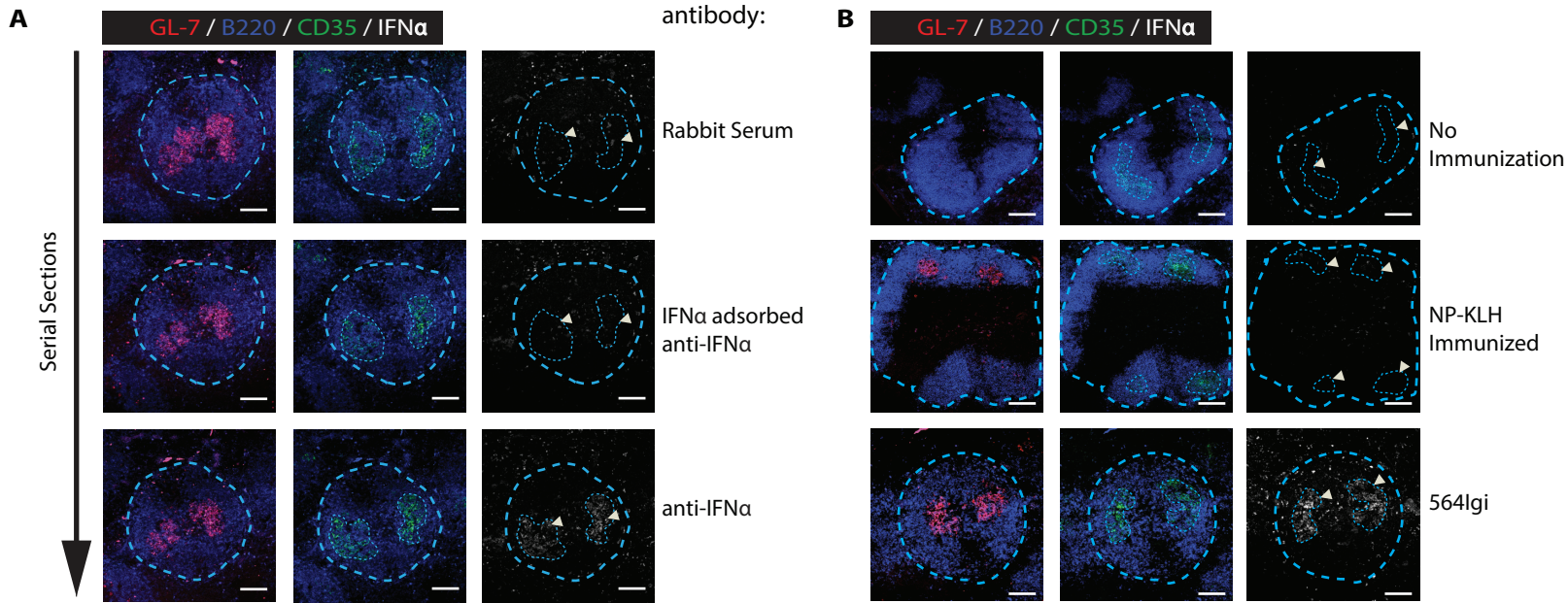


Figure S3

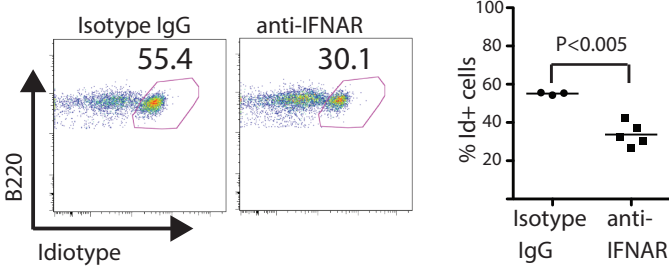


Figure S4

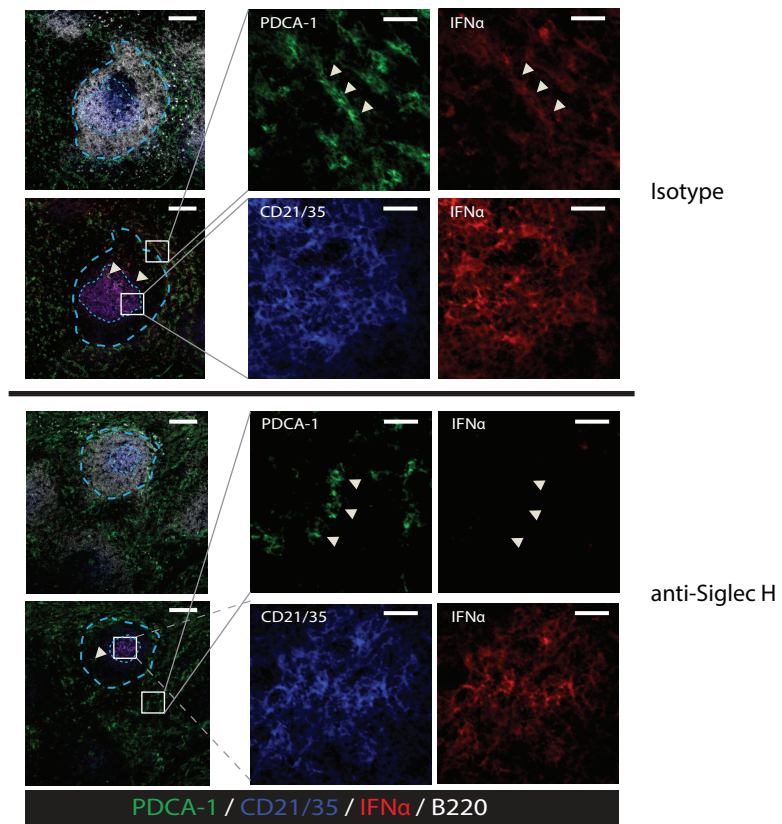


Figure S5

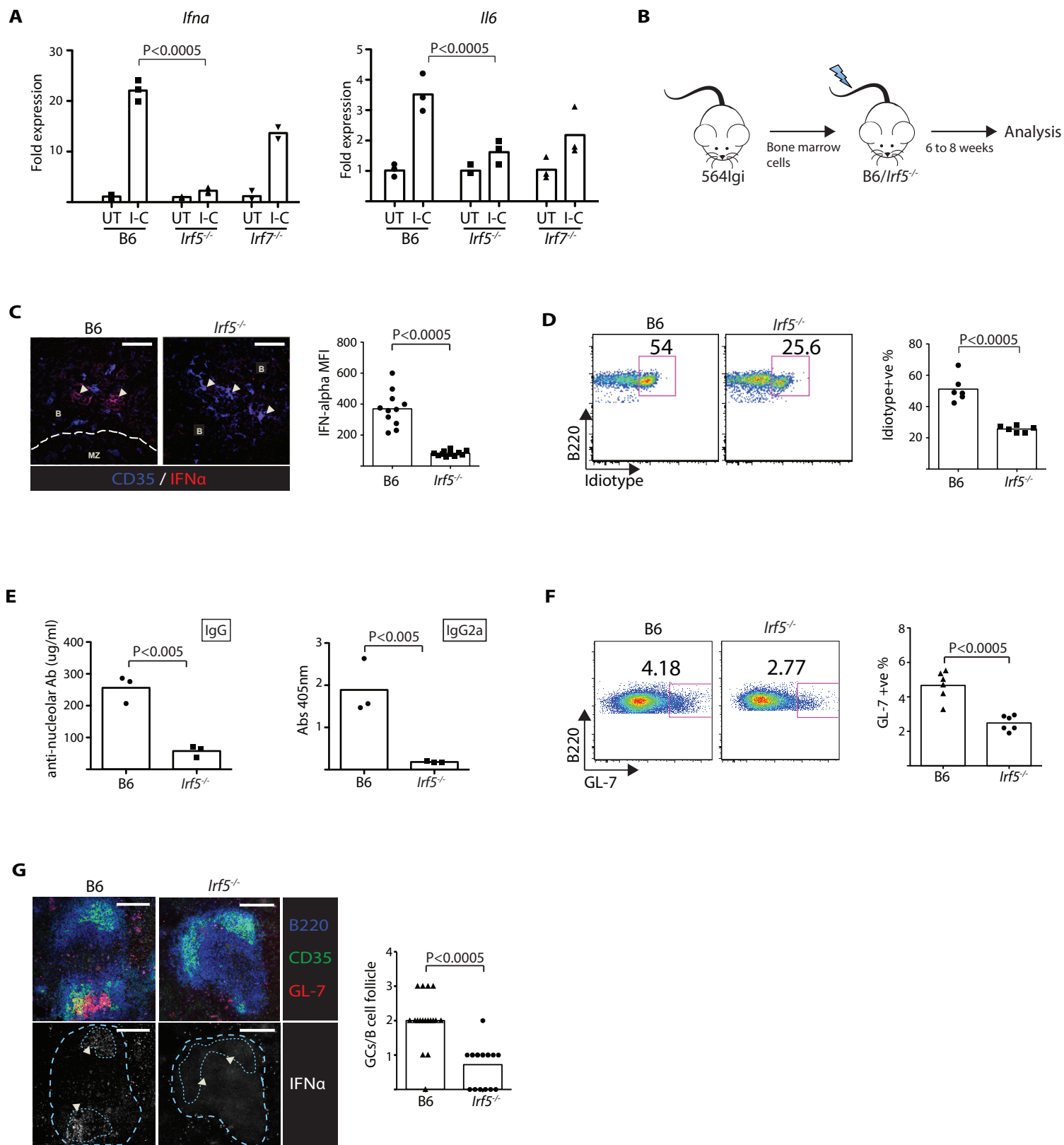
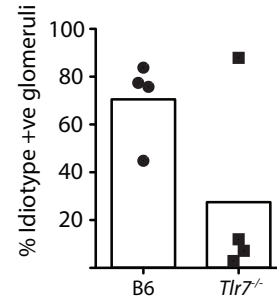
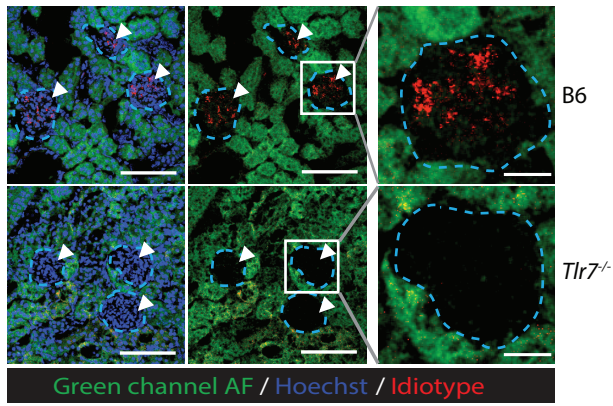


Figure S6



Supplemental Figure Legends

Figure S1. (A) (related to Figure 1) Expression of IFN α by pDCs in spleens of autoimmune 564 Igi mice strain. Spleen cells from B6 or 564Igi mice strains were stained with anti-CD11b, anti-CD11c, anti-PDCA-1 and anti-IFN α and were analyzed by flow cytometer. For analysis of IFN α expression, cells were first gated based on PDCA-1 expression. PDCA-1⁺ cells were identified as pDCs and the PDCA-1⁻ cells were further subdivided into five different subsets based on CD11b and CD11c expression. None of the PDCA-1⁻ subsets showed significant expression of IFN α , both in B6 (not shown) and in 564 Igi. The bottom two plots show frequency of pDCs expressing IFN α in B6 versus 564 Igi. Results show higher frequency of pDCs expressing IFN α in 564 Igi as compared to a B6 WT mouse.

(B) (related to Figure 1) pDCs from B6 and 564Igi mice were sorted based on their phenotype of B220⁺ CD11c^{int} PDCA-1⁺. After RNA extraction, the level of *Ifna* expression was measured using real time PCR. Results show significantly higher expression of *Ifna* (Student's T test, P<0.005) in pDCs from 564Igi as compared to B6, indicating an activated state of pDCs in the 564Igi strain of mice. Data representative of two independent experiments.

(C) (related to Figure 3) FDCs and pDCs isolated from 564Igi mice express higher levels of *Ifna* and *Ifnb1* as compared to total spleen cells. pDCs from 564Igi were sorted based on their phenotype of B220⁺ CD11c^{int} PDCA-1⁺ and FDCs were purified as discussed. For total spleen sample a small piece was directly lysed in Trizol. After RNA extraction, levels of *Ifna* and *Ifnb1* expression were measured by real time PCR. Data show higher expression (One-way ANOVA, N=3) of both *Ifna* and *Ifnb1* by FDCs and pDCs relative to total spleen cells. Tables includes the Ct values of the *Ifna* and *Ifnb1* in the indicated samples. Data representative of two independent experiments.

(D) (related to Figure 3) Enrichment of B220^{-ve} cells in subsequent steps of FDC purification. The three plots show increase in frequency of B220^{-ve} cells in each step of FDC purification. From left; plot shows cells after tissue digestion and prior to magnetic bead based purification of CD21/CD35⁺ve FDCs, cells after the magnetic purification (presort) and cells after sorting (postsort) based on CD21/CD35 and CD157 expression.

Figure S2 (related to Figure 1). **(A)** Control staining with anti-IFN α adsorbed with recombinant IFN α and rabbit serum. Serial sections of spleens from 564Igi were used to stain with rabbit serum, IFN α adsorbed anti-IFN α and anti-IFN α . For adsorbing anti-IFN α with IFN α protein, a mix of 10:1 molar ratio of IFN α protein:anti-IFN α was incubated at room temperature for 30 mins. A common secondary antibody cocktail (anti-CD35, anti-GL-7, anti-B220 and Goat anti-Rabbit) was prepared and used for all the three groups. Data show absence of IFN α staining with rabbit serum and IFN α adsorbed anti-IFN α . Scale indicates 100 μ m. Arrowheads points to FDC regions.

(B) FDCs from mice immunized by NP-KLH (non-nucleic acid antigen) don't express IFN α . Spleen sections from B6, B6 immunized with NP-KLH and 564Igi mice were stained and analyzed for IFN α expression by FDCs. B6 mice were immunized with NP-KLH at day 0 and were given a booster dose on day 22. The spleens were harvested 14 days after the booster dose. Data shows absence of IFN α expression by FDCs in NP-KLH immunized mice in presence of immune response, as observed by the presence of germinal centers. Scale indicates 100 μ m. Arrowheads points to FDC regions.

(C) FDCs in secondary lymphoid organs with access to apoptotic antigens from the small intestine also express IFN α . Mesenteric lymph nodes, Peyer's patches, and inguinal lymph nodes were harvested from B6 or 564Igi mice and tissue sections were stained for B220 (green), CD35 (blue) and IFN α (red). Results show expression of IFN α by FDCs in Peyer's patches and mesenteric lymph nodes both in B6 and 564Igi. FDCs in the skin draining inguinal lymph node from 564Igi mice express IFN α but not those from B6. Scale indicates 100 μ m. The long dashed regions indicate B cell area of the follicle and the short dashed regions mark the FDC network area. Arrowheads points to FDC regions.

Figure S3 (related to Figure 1). Long term treatment of 564lgi mice with anti-IFNAR leads to reduced escape of tolerance of idiotype positive B cells.

564lgi mice were treated for two weeks with anti-IFNAR. The mice were injected with 250µg of the anti-IFNAR or isotype control antibody intraperitoneally on days 0, 4, 8 and 12. The spleens were harvested and analyzed on day14. Anti-IFNAR treatment lead to reduced escape of B cell tolerance as indicated by lower frequency of mature (AA4.1 low) Id+ B cells in anti-IFNAR treated mice (Student's T test, $P < 0.005$). Combined data from two independent experiments with $n=3$ and $n=5$ mice per group in total.

Figure S4 (related to Figure 2). anti-Siglec H treatment does not affect IFN α production by FDCs.

564lgi mice were treated with 500ug of anti-Siglec H i.p. for 4 consecutive days. On day 5 spleen sections were prepared and then stained for B cells (B220, white), FDCs (CD35, blue), pDCs (PDCA-1, green) and IFN α (red). Top panels show B cell follicle from spleen of control isotype antibody treated mice. The bottom panels show data from anti-Siglec H treated mice. Results indicate no loss of IFN α signal in FDCs on anti-Siglec H treatment. By contrast treatment with anti-Siglec H antibody results in significant loss of IFN α signal in pDCs (indicated by arrowheads in the zoomed in images). Arrowheads in the primary images (non-zoomed) indicate pDCs in the white pulp. Scale bars on the first column of images indicates 100µm and those on zoomed in images on the right indicates 20µm. The long dashed regions indicate B cell area of the follicle and the short dashed regions mark the FDC network area.

Figure S5 (related to Figure 5 & 6). Maintenance of autoreactive B cells and autoantibody production is dependent on an intact IRF 5 pathway in stromal cells.

(A) FDCs were isolated from spleens of B6, *Irf5*^{-/-} or *Irf7*^{-/-} mice by magnetic sorting based on CD21 expression on FDCs. 50,000 cells/coverslip were cultured for 7 days after which they were treated with complement opsonized RNP-IC overnight. Immune complexes were generated by mixing nucleoli with 564 anti-RNP in presence of fresh serum. Real time PCR was performed for measuring the *Ifna* and *Il6* expression levels (One-way ANOVA, $N=3$, $P < 0.0005$). Each data point represents technical replicates. Data representative of 2 independent experiments.

(B) Diagram illustrates construction of BM chimeras. *Irf5*^{-/-} or B6 recipients were lethally irradiated and were reconstituted with BM cells from 564lgi mice. B6 served as negative control.

(C) Microscopy images of spleen sections (60X) from the B6 and *Irf5*^{-/-} recipients of 564lgi bone marrow cells (Student's t test, $N=11$, $P < 0.0005$). Scale indicates 50µm. The arrowheads indicate FDC networks. Data representative of two independent experiments. Bar graph shows mean fluorescent intensity (MFI) of IFN α signal. Each data point represents one continuous FDC area.

(D) Flow cytometry plots showing mature idiotype positive B cell frequencies in B6 and *Irf5*^{-/-} recipients (Student's t test, $N=6$, $P < 0.0005$). The plots shown are gated on B220 positive AA4.1 low cells. Each data point represents one mouse. Data representative of two independent experiments. Bar graphs show data pooled from both experiments.

(E) ELISA data showing serum anti-nucleolar IgG (left panel) and IgG2a (right panel) levels in B6 and *Irf5*^{-/-} recipients (Student's t test, $N=3$, $P < 0.005$).

(F) Flow cytometry plots showing GL7+ germinal center (GC) B cell frequencies in B6 and *Irf5*^{-/-} recipients (Student's t test, $N=6$, $P < 0.0005$). The plots shown are gated on B220 positive cells. Data representative of two independent experiments. Bar graphs show data pooled from both experiments. Each data point represents one mouse.

(G) Microscopy images of spleen sections (20X) showing GCs and IFN α signal within FDC network in B6 and *Irf5*^{-/-} recipients (One-way ANOVA, $N=18$, $P < 0.0005$). Scale indicates 200µm. The arrowheads indicate FDC/GC area. GC areas and follicle boundaries are indicated by dotted lines in second row of images. Data representative of two independent experiments. Bar graph shows number of GCs per B cell follicle. Each data point represents one B cell follicle.

Figure S6 (related to Figure 6). Reduced deposition of immune complexes in kidneys of *Tlr7*^{-/-} recipients of 564Igi bone marrow cells.

Kidneys were collected from B6 and *Tlr7*^{-/-} recipients of 564Igi bone marrow cells and tissue sections were stained for nucleus (Blue) with Hoechst and self-immune complexes (Red) with anti-idiotypic antibody. The location of the glomeruli are outlined with dashed line and marked with white arrowheads, with the tubuli green autofluorescence (Green channel AF) encircling the dark glomerular region. This region coincided with the typical cellular dense sphere appearance of the glomerulus observed with the Hoechst nuclear staining in surrounded by the capsular space. The graph on the right shows percent idiotype positive glomeruli in B6 or *Tlr7*^{-/-} recipients. Each data point represents one mouse. Data demonstrates reduced self-immune complex deposition in the glomeruli of most *Tlr7*^{-/-} recipient mice. Scale bars on the first two columns of images indicates 100 μ m and those on zoomed in images on the right indicates 25 μ m.

Supplemental Experimental Procedures

Nucleoli preparation and immune complex generation

Nucleoli were isolated from Raji cells using a previously described protocol (Andersen et al., 2002). Ribonuclear-protein (RNP) immune complexes (ICs) were prepared by mixing 5ul of nucleolar prep with 5ug of 564 anti-RNP (C11 clone, labeled or unlabeled) in GVB++ buffer and in presence of fresh serum from C57BL/6 mice. The mix was incubated at 37°C for 30 minutes, after which it was used for loading FDCs.

Immune complex (IC) purge with anti-CD21

ICs were added to FDC culture and were incubated at 37°C for 1 hour.

After incubation, the medium was removed and fresh medium with anti-CD21 (Clone 7G6) (25ug/ml) or isotype control was added to the culture and was incubated again at 37°C. The removal and addition of fresh medium with anti-CD21 or isotype control was repeated two more times at 2.5 hours and 5 hours after the first anti-CD21 treatment. After the last anti-CD21 treatment, the cells were cultured for additional 11 hours and then fixed-permeablized and stained.

anti-IFN α adsorption

As a control for specificity of anti- IFN α staining, the anti-IFN α antibody was mixed with recombinant mouse IFN α (Biolegend) in a ratio of 10:1 (IFN α protein: anti-IFN α). The mix was incubated at room temperature for 30 minutes before being used for staining spleen sections.

Staining of kidney sections

Kidneys were collected from B6 and TLR7 $^{-/-}$ recipient mice, both transplanted with 564 Igi bone marrow. Kidneys were frozen in optimal cutting temperature (O.C.T.) medium, sectioned at 10 μ m and fixed in acetone. Renal sections from both groups were stained with anti-I δ Ax568. For labeling nucleus in the cells in kidney glomeruli, Hoechst was used at a concentration of 1 μ g/ml. The glomeruli were identified as the dark areas with Hoechst signal, within the tubuli green autofluorescence regions.